Gas Turbine Burner Reactor Network Construction and Application

Thommie Nilsson[1], Cathleen Perlman[1], Harry Lehtiniemi[1],
Daniel Lörstad[2], Sven-Inge Möller[3] and Fabian Mauss[4]

[1]Lund Combustion Engineering – LOGE AB
Lund, Sweden
[2]Siemens Industrial Turbomachinery AB
Finspång, Sweden
[3]Division of Combustion Physics, Lund University
Lund, Sweden
[4]Thermodynamics and Thermal Process Engineering, Brandenburg University of Technology
Cottbus, Germany

1 Introduction

Through the use of a one-dimensional reactor network, quick engineering studies on temperature and fuel effects in gas turbine burners can be performed. A reactor network description of a combustion process allows for the incorporation of flow-field effects observed in three dimensional simulations and enables application of multi-species reaction mechanisms at affordable computational cost. In this paper we report on a novel, automatic reactor network construction methodology for gas turbine burner simulations. The reactor network is constructed using flow-field data from a Reynolds Averaged Navier-Stokes (RANS) Computational Fluid Dynamics (CFD) simulation of a methane Siemens SGT-800 burner [1], operated at a baseline condition. Using homogeneous reactors, the reactor network is used to study the effects of flame temperature and hydrogen content on NO emissions, two properties that were not used for network construction. Stochastic reactors were also applied and the sensitivity on the number of particles and the mixing time constant was investigated. No prior application of stochastic reactor networks in the context of gas turbine burner simulations is known to us.

2 Reactor Network Construction

Several methods for reactor network construction have previously been investigated, all using a flow-field from a CFD calculation as starting point. Fichet et al. [2] and Falcitelli et al. [3] have suggested construction methods based on splitting selected variables into series of intervals. In the method described in [3], several key variables are split and a search for geometrically connected clusters is first performed, giving a large number of reactor network zones. Subsequently, the *N* zones containing the largest number of CFD cells are kept and the cells belonging to the smaller zones are redistributed over the remaining zones. The redistribution of zones is based on minimization of the "unmixedness index" which is essentially the sum of the variances of the variables used for the network generation. This method can produce a predefined number of zones, it can take arbitrary variables into account and good results have been reported. A possible drawback is that some of the zones containing few CFD cells may represent important parts of the domain, not suitable for redistribution. The method in [3] shares the use of field variable variances during the zoning process with the method to be presented here.

Correspondence to: cperlman@loge.se

The method applied in this work differs from that reported in [3] and most other methods in that it performs splitting in linear combinations of (normalized) physical variables. This allows for the consideration of correlations between variables during network construction.

To perform the zonal splitting, a set of relevant field variables are selected. These variables can be for example mixture fraction, species concentrations, reaction progress, velocity components, density, turbulent kinetic energy, eddy dissipation rate and temperature as well as spatial coordinates. The inclusion of spatial coordinates helps to enforce geometrically compact zones.

Given a set of field variables, zones are created through minimization of the variances within the zones. First, dimensionless versions of the selected variables are defined by normalizing them to zero mean and dividing them by reference values, which serve as tolerances. The second step is the application of principal component analysis (PCA) [4] which finds the direction along which the variance of data points is maximized. The data points here are discrete volume elements (CFD cells), so let $\boldsymbol{x}_i = (f_i^1, f_i^2, f_i^3, \dots)$ be a vector containing the normalized field variables $f^1, \dots, f^n$ of cell *i* and m_i be the mass of cell *i*. The direction of maximum variance is then given by the eigenvector $\boldsymbol{u}$ that is associated with the largest eigenvalue of the covariance matrix *R*

$$R = \frac{1}{N}\sum_{i=1}^{N} m_i \boldsymbol{x}_i \boldsymbol{x}_i^T \tag{1}$$

where *N* is the number of cells in the set. A split location is selected along the direction defined by this eigenvector such that the sum of variances for the resulting zones is minimized. To do so, the coordinates $c_i = \boldsymbol{u} \cdot \boldsymbol{x}_i$ in this direction are computed and sorted, all *N – 1* splitting possibilities are tested, and the one which gives the smallest total variance is selected. The procedure is repeated by selecting the zone with the largest variance, applying the PCA and splitting it. The process is terminated when all zones fulfill an interval based stopping criterion. In this work the maximum interval *I* over all directions representing the pure cluster variables was used:

$$I = \max_q(\max_i x_{i,q} - \min_i x_{i,q}). \tag{2}$$

Here *i* runs over all cells in the zone and *q* runs over all variables. The splitting procedure may result in geometrically disconnected zones so a further splitting of disconnected zones is needed. This additional splitting, which is based on connectivity, usually results in small zones containing only one or two CFD cells. To avoid this, all zones with less than a certain number of cells are redistributed. What zone a CFD cell is moved to is decided by the requirement of connectivity and the smallest violation of the zone division stopping criterion.

Once the zoning is performed, the mass flux between zones is extracted from the CFD flow-field using the net flux for each connected cell-face pair.

3 Results and Discussion

Baseline calculations and sensitivity: The baseline reactor network was constructed from an axisymmetric RANS simulation of the SGT-800 burner in a combustion rig [5]. For the CFD simulation, the commercial CFD solver STAR-CD v. 4.20 [6] was used together with the well-stirred reactor combustion model of LOGEsoft [7]. A mechanism for methane combustion containing 28 species, obtained through the reduction of the detailed 163 species C1-C4 mechanism from Schenk et al. [8], was used.

To find out how many reactors or how strict tolerances are needed to get a good network, a number of networks were constructed using the baseline tolerances specified in Table 1, multiplied by a factor. These networks were simulated using the same 28 species mechanism that was used in the CFD calculations and CO concentration and temperature at the outlet were compared. Variables used for the PCA and their corresponding baseline tolerances are summarized in Table 1. It should be noted

that both CO and temperature were used in the network construction. The baseline network consists of 148 zones.

Figure 1 shows normalized calculated CO as function of tolerance scaling factor and the corresponding number of resulting zones. Outlet CO is generally insensitive since CO is consumed near the flame front and mostly constant in the post-flame, making it independent of post-flame resolution. However, for very low resolution networks the error increases considerably as also the flame front loses resolution.

Table 1. Variables used for PCA-based network construction.

Variable	**Tolerance**	**Variable**	**Tolerance**
x and y coordinates	40 mm	CH_4 mass fraction	$2.0 \cdot 10^{-3}$
x-velocity	40 m/s	OH mass fraction	$5.0 \cdot 10^{-4}$
y-velocity	20 m/s	O_2 mass fraction	$3.0 \cdot 10^{-2}$
Temperature	120 K	CO mass fraction	$1.0 \cdot 10^{-3}$
Density	0.05 kg/m^3	Minimum number of cells	3

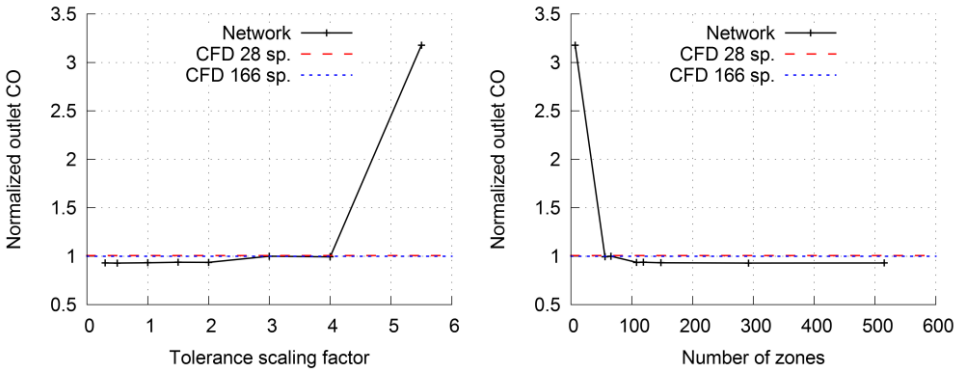

Figure 1. Effect of tolerances (left) and number of zones (right) on predicted CO emission.

The outlet temperature difference between the finest (515 zones) and the coarsest (7 zones) networks was 0.1%. Outlet temperature is insensitive to the network resolution since the combustion is complete in terms of heat release and as heat transfer through the reactor walls is not modelled. Outlet temperature is thus not an interesting variable to look at on its own but its insensitivity is helpful when investigating the highly temperature-dependent NO formation chemistry.

To check the sensitivity of NO formation to network construction a study was made where a scaling factor was applied only to the tolerances for spatial coordinates, leaving all other tolerances at their baseline values. The baseline network was used and Figure 2 shows the results of these calculations compared to experiments and a CFD calculation. The Schenk et al. [8] mechanism augmented with extended Zeldovich NO chemistry, resulting in 166 species, was used in both the network and in the CFD calculation to which the network results are compared.

The two different experiments in Figure 2 refer to measurements for the same operating condition using two different burners of the same type. The reactor network NO prediction is somewhat affected by relaxed tolerances and by a decrease in number of zones. The difference between the CFD calculation and the different networks is small, considering the reduction in computational complexity. It should be noted that the reactor network was constructed based on the CFD calculation performed with the 28 species mechanism.

Flame temperature effect on NO emission: The effect on outlet NO was investigated using the baseline reactor network with the 166 species mechanism. Different flame temperatures were obtained by varying the fuel/air ratio at the network inlet. In the corresponding experiments only the inflow rate of fuel was varied but this has only a small effect on the overall mass flow rate since only 2-3 % of the total mass is fuel. Figure 3 (left) shows normalized NO mass fractions as function of flame

temperature. The rate at which NO increases is somewhat over-predicted but the trend is in agreement with the experiment.

Hydrogen effect on NO: The effect of adding hydrogen to the fuel was investigated by Lantz et al. [9]. The reactor network based on the pure methane CFD simulation with the 28 species mechanism was used in an effort to reproduce the observed trends and the sensitivity of outlet NO when hydrogen is mixed into the fuel stream. Both in experiments and simulations [9] the fuel inflow rate was adjusted to maintain a constant temperature over the range of hydrogen concentrations. It was reported in [9] that the whole flame front moves upstream with increasing hydrogen content. This may affect the flow pattern around the flame, thus limiting how well the network can extrapolate from pure methane, both because a higher error is introduced in the zone-to-zone flow but also because the network was constructed from a CFD simulation with a certain flame position. However, if chemical effects are dominant the network may still be able to reproduce the trend of NO formation. The hydrogen concentrations used in the reactor network were 0, 20, 40, 60, 80 and 100 mol-%. Figure 3 (right) shows normalized outlet NO calculated with the baseline reactor network, using homogeneous reactors and the GRI-mechanism [10], the Schenk et al. [8] mechanism augmented with Zeldovich NO (166 species) and with NO chemistry from the GRI-mechanism (180 species) compared to results of two experimental measurements for the same operating conditions. The experimental results are from two physically different burners of the same type. Considering only chemical effects, different NO levels for varying hydrogen content are expected due to prompt NOx formation, which is a result of reactions between nitrogen gas and radicals. In a burner also geometrical effects, such as flame shape and position, can affect NO formation.

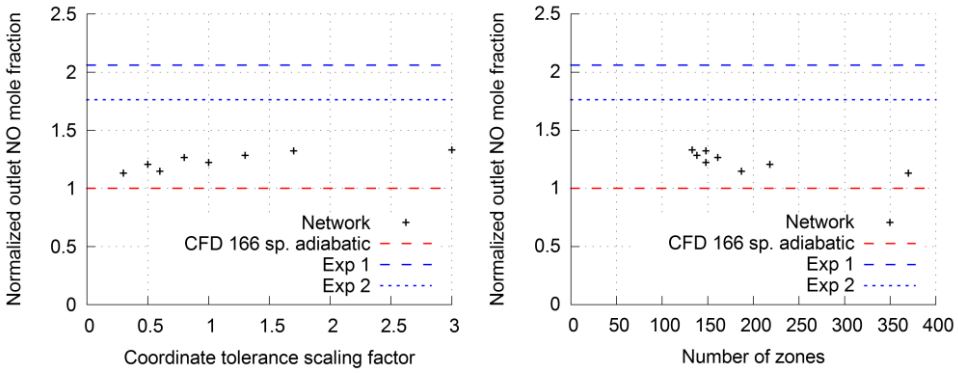

Figure 2. NO sensitivity as function of coordinate tolerance scaling factor (left) and number of zones in the reactor network (right).

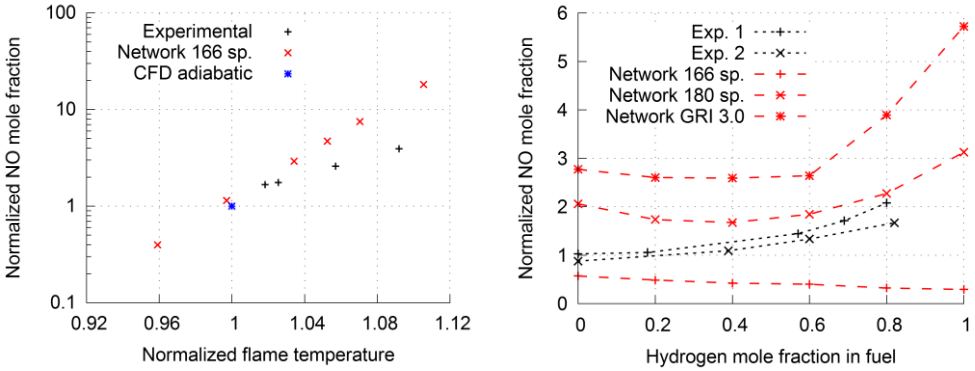

Figure 3. Effect of flame temperature on NO emission (left) and normalized outlet NO in network simulations of the Siemens burner rig using three different mechanisms as function of H2 content in the fuel mixture (right).

The 166 species mechanism does not include prompt NOx and does therefore not predict any change in NO with increasing hydrogen. For the other mechanisms a change in slope around 60 % hydrogen and an increasing NO concentration is visible. A slight change in slope can be seen also in the experimental data but said change is clearly over-predicted in the simulations. We have however observed that in the 80 % and 100 % hydrogen network simulations the flame front makes a jump upstream in the simulations (not shown here), almost into the burner, making the flame region smaller and the post-flame larger, which may have an effect on NO formation. This jump happens for all mechanisms but does not notably affect the case with only thermal NOx. It may however be part of the reason that the other cases predict such a big change in slope.

Stochastic reactor calculations: The central questions for the stochastic reactors [11] are how many particles and what mixing time to use. It is important to settle the different nature of these two parameters. The mixing time is a measure of how homogeneous the reactor is ($\tau_{mix} \rightarrow 0$ corresponds to a homogeneous reactor) and is thus a physical quantity, typically related to the integral mixing timescale (calculated in the CFD simulation) through a constant $\tau_{mix} = \tau_{turb}/C_{\Phi}$. Particle number is a measure of the resolution of a reactor in the numerical model; it is thus not a physical quantity and should ideally be as high as possible. A stochastic reactor with only one particle may behave just like a homogeneous reactor but this does not mean low particle numbers give more homogeneous reactors in general, any effect of low particle numbers are discretization errors. A stochastic reactor with very few particles is thus expected to perform worse than a homogeneous reactor.

To determine how many particles are needed a parameter study was carried out. Network calculations were done with 5, 15, 25, 40, 55 and 100 particles per zone using the 28 species mechanism. The difference in temperature when going from 55 to 100 particles was no more than 30 K for any zone with most zones differing less than 15 K. Therefore the 100 particles case was used as reference. Differences in temperature compared to the other cases are shown in Figure 4a.

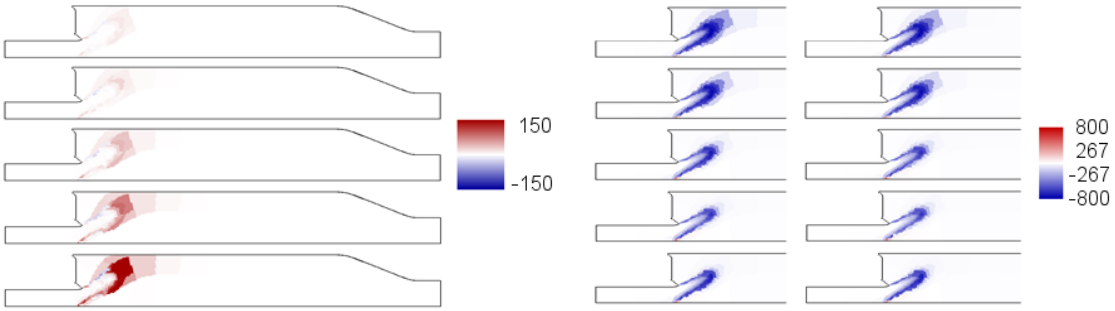

Figure 4. (a) Temperature difference in K when using 5 (bottom), 15, 25, 40 and 55 (top) particles per reactor compared to using 100 particles. The baseline network with 148 zones has been used; (b) Temperature difference in K between CFD and stochastic reactor network simulations. Mixing time scale factor C_{Φ} from top to bottom: 1, 2, 10, 20 and 50. Curl mixing model (left) and modified Curl mixing model (right).

To investigate the effect of the mixing time constant C_{ϕ}, networks were calculated for C_{Φ} = 1, 2, 10, 20 and 50. Figure 4b shows a comparison between the baseline CFD simulation (mass-weighted averages within each zone) and network simulations using 55 particles per reactor and either Curl [12] or modified Curl [13] mixing. Note that most of the error is made up of zones that are too cold due to the flame being too far downstream. It is ensured that C_{ϕ} gives the same variance decay rate in both mixing models. Table 5 summarizes the largest positive and negative difference and the root-mean-square (RMS) difference between the networks and the CFD simulation. The homogeneous reactor network is also included for comparison. RMS was calculated without any weighting as all network zones are considered equally important. Best results were obtained around $C_{\phi} = 20$. The error increases for both more (higher C_{ϕ}) and less (lower C_{ϕ}) mixing. Modified Curl mixing was better in

all cases tested, which is consistent with the continuous probability density function produced by the modified Curl model [14].

Table 5. Largest positive and negative difference and RMS difference between the stochastic networks and the baseline CFD for the Siemens burner rig.

C_φ	Curl mixing model		Modified Curl mixing model	
	Deviation [K]		Deviation [K]	
	min/max	RMS	min/max	RMS
1	+434 / -792	382	+436 / -783	371
2	+449 / -773	363	+456 / -764	353
10	+469 / -713	310	+471 / -641	271
20	+471 / -635	262	+472 / -624	249
50	+472 / -715	313	+471 / -713	312
-	+470 / -749	338	Homogeneous reactor network	

4 Conclusion

An algorithm for reactor network construction based on principal component analysis was developed. A sensitivity study on the tolerances used by the algorithm and on the number of zones was performed. It was found that results close to the CFD solution can be achieved.

The reactor network, which was generated using a baseline CFD calculation, was applied to two investigations of NO emission: (1) effect of flame temperature and (2) effect of hydrogen enrichment of the fuel stream. It was found that the reactor network was able to predict the trend due to flame temperature but the effect on NO emission from hydrogen enrichment in the fuel stream proved more difficult to capture. It appears that the effect of prompt and thermal NO formation is prominent. In addition, the choice of chemical mechanism may affect the prediction and ideally a mechanism validated for NOx formation for the proper range of methane/hydrogen mixtures should be used.

An investigation of the effect of mixing time constant, number of particles and mixing model for a stochastic reactor network was also performed. It was found that the modified Curl mixing model performs better than the standard Curl model and that the mixing time constant $C_\phi = 20$ produced overall best results. The number of particles per reactor needs not exceed 55.

ACKNOWLEDGEMENT The authors thank Dr. Rajesh Rawat, CD-adapco, for providing the STAR-CD license used in this work.

References

[1] Lörstad D et al. (2013). ASME Turbo Expo 2013, Paper GT2013-95478.
[2] Fichet V et al. (2010). Fuel, 89(9):2202-2210.
[3] Falcitelli M et al. (2002). Combust. Sci. Technol. 174(11-12):27-42.
[4] Jolliffe, IT (1986). Principal component analysis, Springer-Verlag, Berlin.
[5] Lörstad D et al. (2010). ASME Turbo Expo 2010, Paper GT-2010-22668.
[6] CD-adapco (2013). Methodology – STAR-CD v. 4.20.
[7] LOGE AB (2014). http://www.loge.se/Products/Products.html
[8] Schenk M et al. (2013). Combust. Flame 160(3):487-503.
[9] Lantz A et al. (2014). ASME Turbo Expo 2014, Paper GT2014-26293.
[10] Smith GP et al. GRI-mech v. 3.0, http://www.me.berkeley.edu/gri_mech/ accessed Jan. 2014.
[11] Kraft M et al. (2000). Proc. Combust. Inst. 28:1195-1201.
[12] Curl RL (1963). AIChE J. 9 (2):175-181.
[13] Janicka J et al. (1979). J. Non-Equil. Thermodyn. 4(1):47-66.
[14] Haworth DC (2010). Prog. Energy Combust. Sci. 36:168-259.